EARTH SCIENCES
RESEARCH JOURNAL

Earth Sci. Res. J. Vol. 20, No. 4 (December, 2016): B1 - 10

UNIVERSIDAD NACIONAL DE COLOMBIA
SEDE BOGOTÁ
FACULTAD DE CIENCIAS
DEPARTAMENTO DE GEOCIENCIAS
RESEARCH GROUP IN GEOPHYSICS

GEODYNAMICS

The geological and geodynamic condition on the formation of the Dabashan thrust nappe structure: Based on FLAC numerical modelling

Xiaoning Zhang*, Yunpeng Dong.
State Key Laboratory of Continental Dynamics, Department of Geology, Northwest University. China.
*Corresponding author: xiaoningdev@gmail.com

ABSTRACT

The Dabashan thrust nappe structure at the southern margin of the Qinling orogenic belt suffered at least two stages of evolution which are Late Triassic plate subduction collisional orogeny between North China block, Qinling micro-plate and Yangtze block followed by intracontinental orogeny since the Meso-Cenozoic. A prominent topography characteristic within the Dabashan area is a southwestward extrusive arc (Bashan Arc fault) that is one of key factors to understand the geodynamic condition of the Dabashan thrust nappe structure.

In this work, two-dimensional plan-view models are constructed to simulate the collisional and intracontinental orogenic movements, and the factors that may control the formation of the Bashan Arc fault are analysed. The modelling results show that the compressive stress produced by the plates collision along both north and south boundaries is the main driving force. The dextral shearing derived from the inconsistent shape on the block margins is the main controller. Rigid tectonic units such as Bikou and Hanan-Micangshan terranes, Foping and Wudang domes, as well as Shennongjia-Huangling anticline also contribute as "anchor" effects. Additionally, the rheology properties of rock material in the Dabashan area affect the shape of the arc.

Keywords: Numerical modelling; South Qinling; Bashan Arc; Dabashan; Thrust nappe structure

Condición geológica y geodinámica para la formación estructural de la falla de cabalgamiento en las montañas Dabashan basada en el modelo numérico del software FLAC

RESUMEN

La estructura de la falla de cabalgamiento de las montañas Dabashan en el margen sur del cinturón orogénico de Qinling sufrió por lo menos dos etapas de evolución, la colisión orogénica del Triásico Superior entre el bloque de la China del Norte, la microplaca de Qinling y el bloque Yangtze, y la orogénesis intracontinental desde el Meso-Cenozoico. Una característica topográfica prominente del área de Dabashan es un arco extrusivo (falla Arco de Bashan) hacia el suroeste, que es un factor determinante para entender la condición geodinámica de la falla de cabalgamiento en las montañas Dabashan. En este trabajo se construyeron modelos bidimensionales planos para simular los movimientos de colisión e intracontinental orogénicos y se analizaron los factores que podrían controlar la formación de la falla del Arco de Bashan. Los resultados del modelado muestran que el esfuerzo de compresión producido por las placas de colisión en los límites norte y sur es la principal fuerza impulsora de la falla. La principal controladora es la fuerza de cizallamiento dextral derivada de la forma inconsistente en los margenes del bloque. Las unidades tectónicas rígidas como los terrenos Bikou y Hanan-Micangshan, el domo Foping y Wudang, al igual que el anticlinal Shennongjia-Huangling tienen funciones de ancla. Adicionalmente, las propiedades reológicas del material rocoso en el área Dabashan afectan la forma del arco.

Palabras clave: Modelado numérico, Qinling Sur, Arco Bashan, montañas Dabashan, falla de cabalgamiento.

Record

Manuscript received: 05/07/2013
Accepted for publication: 11/11/2016

How to cite item
Zhang, X., & Dong, Y. (2016). The geological and geodynamic condition on the formation of the Dabashan thrust nappe structure: Based on FLAC numerical modelling. *Earth Sciences Research Journal, 20(4), B1-B10*
http://dx.doi.org/10.15446/esrj.v20n4.38666

ISSN 1794-6190 e-ISSN 2339-3459

http://dx.doi.org/10.15446/esrj.v20n4.38666

1. Introduction

The Qinling orogenic belt is located at center China, between the South China and North China blocks (Fig. 1a). It is at a key tectonic position, been considered as a composite orogenic belt, formed by the collision of the South China and North China blocks (Mattauer et al., 1985; Sengor, 1985; Zhang, 1985; Ren et al., 1986; Hsu et al., 1987; Zhang et al., 1987, 1989; Enkin et al., 1992; Kröner et al., 1993; Li et al., 1993; Okay and Sengor, 1993; Ames et al., 1996; Zhang et al., 1996a; Hacker et al., 1998; Meng and Zhang, 1999; Faure et al., 2001; Zhang et al., 2001; Ratschbacher et al., 2003, 2006; Dong et al., 2011a,b,c, 2012a,b; Bader et al., 2013a,b; Dong et al., 2013; Li et al., 2015; Dong et al., 2016). Qinling orogenic belt has preserved a lot of kinematic evolution records of long-term multiple stages subduction and collision between the South China and North China blocks, as well as tectonic records of overthrust thrusting, strike-slip regulation, extensional collapse, been a good region for studying orogenic tectonic process.

The Dabashan thrust nappe structure is one of major characteristics of Qinling orogenic belt. It is located between Hannan and Shennongjia-Huangling terranes (Fig. 1b,c), as a part of the southern margin of South Qinling thrust nappe structure (Fig. 1a, Dong et al., 2008; Shi et al., 2013). The Dabashan thrust nappe structure is suggested as the result of the subduction collision between North China Block and Yangtze Block combined Mesozoic-Cenozoic intracontinental orogeny of Qinling orogenic belt (Fig. 1a, Zhang et al., 2001; Ratschbacher et al., 2003; Wang et al., 2003; Dong et al., 2008). It's geological and geodynamic evolution has been one of research hotspots over the past decades, lots of study results have been reported in this area (e.g. Cai et al., 1988; He et al., 1997, 1999; Zhang et al., 2001, 2010; Wang et al., 2003; Dong et al., 2005, 2006, 2008, 2011; Li et al., 2006; Liu et al., 2006; Wang et al., 2006; Shi et al., 2007, 2012, 2013; Tan et al., 2007; Hu et al., 2009, 2012).

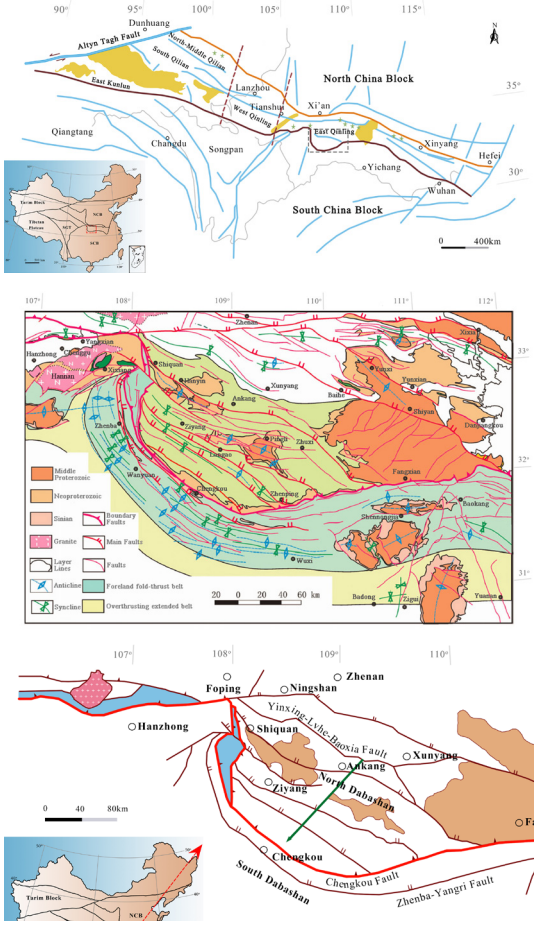

Figure 1. Schematic map of the research area. (a) The large-scale structural units sketch within China (Zhang et al., 2001). (b) The Bashan Arc thrust nappe structure (Dong, et al., 2008). (c) The regional scale structural sketch within the research area (Zhang et al., 2001).

The Bashan Arc is one of key factors to understand the geodynamic evolution of the Dabashan thrust nappe structure. There are different evolution models about Bashan Arc. Jiang et al (1982) emphasizes the similar shape and structure between the Bashan Arc and the Himalayan Arc and believes that the intruding of Hannan and Huangling terranes together with the lateral movement are the main geodynamic condition of the Bashan Arc. Xu et al (1988) points out that the southward huge thrust and detachment shear of South Qinling is the main geodynamic condition while Hannan and Huangling terranes play roles of baffles. Zhang et al (2001) and Wang et al (2003) think that the subduction from south to north of the Yangtze Block may also play an important role within the Bashan Arc. Dong et al (2008) suggests that Yanshanian intracontinental overthrusting from south to north developed the Bashan Arc. Zhang et al (2010) and Wang et al (2011) estimate that the pre-formed Chengkou-Fangxian fault is the key controller to Bashan Arc. He et al (1997) proposes an extrusion shear model that stresses the importance of the dextral shear in the Dabashan area. In additional, durative compression model (Cai et al., 1988), slip layer controlling model (Li et al., 2006; Liu et al 2006), bulldozer model or progressive squeeze weakened model (Luo et al., 2007), two phases model (Dong et al., 2006) are also suggested.

Despite many studies reported within this area, there are still disagreements on below issues: 1) is there dextral strike-slip around the Bashan arc fault? How it formed and effected on the evolution of Dabashan thrust nappe? 2) Did Shennongjia – Huangling and Bikou terranes play a role of "rigid anchor" in the formation of the Dabashan thrust nappe? 3) Did collision between Yangtze and North China blocks cause clockwise rotation within Dabashan area, and how that effect the formation of Dabashan thrust nappe? This paper presents a numeric modelling using Fast Lagrangian Analysis of Continua algorithm (FLAC) to analyse the geodynamic evolution of the Dabashan thrust nappe and the formation of the Bashan Arc, and mainly focuses on above issues.

2. Tectonic setting

The Dabashan thrust nappe structure is at the northeastern of the Sichuan basin and the northwestern of the central Yangtze block (Zhang et al., 2010, Shi et al., 2013), characterized as an obvious southwestward arc and distinguished with the Qinling-Dabie orogenic belt (Fig. 1b, Zhang et al., 2001; Dong et al., 2006, 2008, 2013; Shi et al., 2012, 2013). The Dabashan thrust nappe structure can be divided into Southern and Northern Dabashan tectonic units which are evidently different (Fig. 1c, Zhang et al., 2010; Shi et al., 2012, 2013), the Northern Dabashan tectonic unit shows NW-SE direction while Southern Dabashan tectonic unit spreads as arc shape and displays features of two stage overprint (Dong et al., 2008). From view of lithology, the Southern and Northern Dabashan tectonic units are also distinct (e.g. Middle Proterozoic Shennongjia Group, Sinian Nantuo-Doushantuo-Dengying formations, Cambrian sandstone-shale-carbonate for Southern Dabashan unit while Middle-Neo Proterozoic Wudang Group and Yunxi Group, Neoproterozoic Yaolinghe Group, Cambrian slate-carbonate for Northern Dabashan unit and so on), they belong to different origin sources and were overlaid by southward thrust nappe movement (Dong et al., 2008).

The Northern Dabashan unit consists of a few thrust nappes with multiple levels and different scales that stacked southward and mainly characterized by series of NW-SE faults and folds. The main structural trend is about 290°~300° paralleling to that of Qinling. The southern front of the Northern Dabashan, close to Bashan Arc fault, featured by folds with south-dipping axial planes, is evidently different with dominant north-dipping axial planes in both North and South Dabashan units, indicating that the Northern Dabashan underwent at least two stages of thrust movements (Zhang et al., 2001; Dong et al., 2008; Zhang et al., 2010). These folds with south-dipping axial planes should be formed at the early stage of collision and overprinted by following southward thrust nappes. The total shortening in the Northern Dabashan may reach 31%~48% (Dong et al., 2008).

The Southern Dabashan unit is located at the northeastern margin of Sichuan basin, with two rigid basements (Hannan-Micangshan and Huangling-

Shennongjia massifs) in its east and west sides (Fig. 1b,c, Zhang et al., 2001; Dong et al., 2006, 2008, 2011; Shi et al., 2012, 2013). The unit displayed as a typical double arc-shape structure in the west flank of the Huangling-Shennongjia massif (Yue et al., 1996; Huang 2000; Wu et al., 2009; Shi et al., 2012, 2013). The Southern Dabashan is characterized by developed fold-thrust structures, can be further divided into northern foreland fold-thrust belt and southern overthrusting extended belt (Fig. 1b). The former displays overprinting of two stage folds where different hinge trends indicate earlier dextral shear and later thrust superposition. The latter mainly consist of thin-skinned folds, characterized by upright and wide folds with few faults. It seems that the structural deformation in the Southern Dabashan is gradually weakened from northeast to southwest and the average shortening is about 36%~53% (Dong et al., 2008).

The Bashan Arc fault constitutes a boundary between the Southern and Northern Dabashan tectonic units (Zhang et al., 2001; Dong et al., 2008; Zhang et al., 2010). In fact, it is a thrust nappe belt consisting of a series of NE-SW or N-S thrusts. The major nappe fault was suggested to be associated within the Chengkou fault that formed and been active during Middle - Late Jurassic (Xu et al., 2005). The general movement of the Bashan Arc fault is towards southwest (240º). The vanguard portion, e.g. Chengkou section, is nearly parallel with the structural trend of the North Dabashan (about 290°~300º) while west and east sides cut the structural line of the North Dabashan with high angles (Dong et al., 2008).

Hannan-Micangshan terrane, Foping dome, Shennongjia-Huangling terrane, as well as Wudang dome, located at the southwest, northwest, southeast, and northeast of the Bashan arc fault belt respectively (Fig. 2), were supposed as the "anchor" during the formation of the Dabashan thrust nappe structure because of their relative rigid basements (Dong et al., 2008; Zhang et al., 2010; Wang et al., 2011). Along with the activity of the Bashan arc fault, they might work together to play an important role to construct the current structural styles of the Dabashan thrust nappe.

Bikou terrane, surrounded by Qingchuan-Yangpingguan fault and Mianlue suture belt, located at the northwest of the Dabashan thrust nappe, was supposed intruded into the South Qinling and also contributed to the formation of the Dabashan thrust nappe.

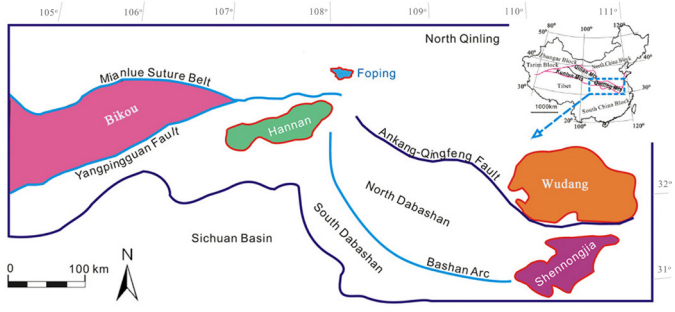

Figure 2. Simplified geometry map of the research area. The map in upper-right corner indicates the location of the research area within China (Dong et al., 2011b).

3. Numerical method

3.1 Model description

A two-dimensional (2D) plan-view model (Fig. 2, 3) was designed to simulate the formation of the Bashan Arc, and mainly focused on the condition that leads to the Bashan fault bending. According to previous studies (e.g. Jiang et al., 1982; Xu et al., 1986; He et al., 1997, 1999; Zhang et al., 2001; Wang et al., 2003; Dong et al., 2006; Li et al., 2006; Liu et al., 2006; Luo et al., 2007; Dong et al., 2008; Zhang et al., 2010; Dong et al., 2011b; Wang et al., 2011, 2013), we assume that the bending conditions might include: 1) the North Qinling moves towards south; 2) the Yangtze Block moves towards north; 3) the irregular margin of blocks produces dextral shearing and lateral extrusions in Dabashan area; 4) Hannan-Micangshan terrane, Foping dome, Shennongjia-Huangling anticline, as well as Wudang dome act as baffles to hold down the thrust nappe (Fig. 2). Although Bikou terrane is a little far from Bashan Arc Fault, it is at the north of the northeast margin of Sichuan basin, and very close to possible model boundary, we included it as one of experiment steps. The geometry in the 2D plan-view model is based on the reconstruction of above tectonic units, Bashan Arc fault, as the focus of the model, is designed as a straight line at the initial stage, while the North Qinling and the Sichuan Basin, playing roles of parts of the boundary conditions, are moved to outside of the model boundaries (Fig. 3) except for stresses or velocities applied on their south margin and northeast margin, respectively.

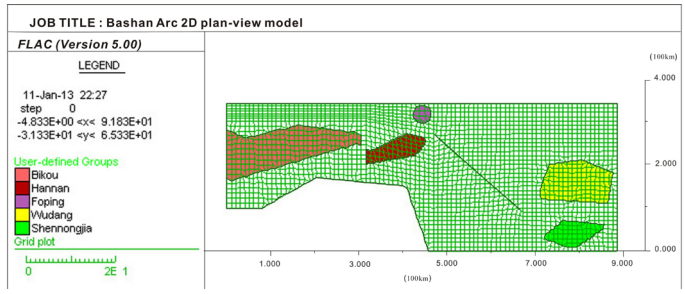

Figure 3. The geometry units and finite difference mesh for 2D plan-view model.

Detailed model parameters, such as rock properties, boundary and initial conditions are the key factors for numeric models and should be adjusted during model solving, they will be discussed in the numerical result session.

3.2 Numerical algorithm

The commonly used numerical algorithm for geology modelling can be divided into 3 groups which are: 1) continuum methods that include Finite Difference Method (FDM) and Finite Element Method (FEM), as well as Boundary Element Method (BEM); 2) discontinuum methods that include Discrete Element Method (DEM) and Discrete Fracture Network (DFN); 3) hybrid methods that combined continuum and/or discontinuum methods (Jing, 2003).

FLAC is one of FDM algorithm with the mixed-discretization technique (Cundall and Board, 1988; Itasca, 2005). It has been widely used to simulate rock deformation (Xia et al., 2006) and solve structural geology problems (Hobbs et al., 1990; Ord, 1991; Zhang et al., 1996b; Zhang et al., 1996c; Zhang et al., 2000; Strayer et al., 2001). For example, Ord (1991) simulated the uniaxial compression deformation of Gosford sandstone and demonstrated that the stress-strain relationships from the FLAC numerical models for several different confining pressures are consistent with those reported from an experimental work (Edmond and Paterson, 1972).

Similar to most mesh-based numerical modelling methods, materials (geology blocks, rocks and so on) in FLAC are represented by elements, or zones, which form a grid. Each grid is assigned material properties, such as density and elastic moduli, and behaves according to a prescribed linear or nonlinear stress/strain law in response to the applied forces or boundary restraints (Itasca, 2005; Xia et al., 2006). The material can yield and flow, and the grid can deform in large-strain mode and move with the material that is represented.

Using the explicit and Lagrangian calculation scheme, together with the adapted mixed-discretization technique, FLAC ensures that material failure and large deformation are modeled accurately. The explicit method and dynamic relaxation scheme make it possible to carry out large calculations with relatively less memory requirements because of no global stiffness matrix formed during computation. However, the time-step must be small enough to ensure convergence and numerical stability (Cundall and Board, 1988).

FLAC contains a powerful built-in programming language FISH (short for FLACish, Itasca, 2005) that can be used to extend FLAC's functionality, e.g. generate very complicated geology bodies, apply any kind of initial and boundary conditions, or implement special constitutive models for any materials.

In this study, we select FLAC as the major numerical modelling platform and use FISH to implement most of numerical algorithm and functionalities.

3.3 Theoretical basis

The elastic-viscous constitutive law (known as the Maxwell substance, Itasca, 2005) can be used to simulate the time-dependent behavior of materials that exhibit creep, for example, the irrecoverable deformation of rocks under small stresses and over a long period. An elastic-viscous rheology material exhibits both viscous and elastic behaviors (Itasca, 2005). It is equivalent to a combination of an elastic element and a Newtonian viscous element in series (Turcotte and Schubert, 1982; Ranalli, 1987), in which the instantaneous elastic response and the viscous deformation are coupled (Xia et al., 2006). The total strain (ε_{ij}) is the sum of the elastic strain (ε_{ij}^{e}) and viscous strain (ε_{ij}^{v}),

$$\varepsilon_{ij} = \varepsilon_{ij}^{e} + \varepsilon_{ij}^{v} \tag{1}$$

The elastic strain relates to stress (σ_{ij}) according to Hooke's law

$$\sigma_{ij} = 2G\varepsilon_{ij}^{e} + (K - \frac{2}{3}G)\delta_{ij}\varepsilon_{kk}^{e} \tag{2}$$

where G, K and δ_{ij} re shear, Hand the Kronecker delta, respectively, and the viscous strain rate ( ) relates linε_{ij}^{v} to stress according to the Newtonian flow law

$$\sigma_{ij} = 2\eta\varepsilon_{ij}^{v} - \frac{2}{3}\eta\delta_{ij}\varepsilon_{kk}^{v} \tag{3}$$

Where η is viscosity. Strain rate is defined as a function of velocity gradients.

The elastic–plastic constitutive law (Mohr–Coulomb model, Itasca, 2005) is the conventional model used to represent shear failure in soils and rocks. Vermeer and DeBorst (1984) report laboratory test results for sand and concrete that match well with the Mohr-Coulomb criterion. A Mohr–Coulomb elastic–plastic material undergoing deformation behaves initially elastically until the stress reaches a critical value known as the yield stress, at which point it begins to deform plastically, and irreversibly, to high strain (Xia et al., 2006). The yield of such material may be expressed as a yield function f , given by

$$f = \tau_m + \sigma_m \sin\phi - C\cos\phi \tag{4}$$

where τ_m is the maximum shear stress, σ_m is the mean stress, ϕ is the friction angle and C is the cohesion. The material is in an elastic state if $f < 0$ (the stress state is not touching the yield surface), and is in a plastic state if $f = 0$ (the stress state is touching the yield surface) (Xia et al., 2006). Detailed information on using the Mohr–Coulomb elastic–plastic materials to simulate deformation in thrust wedge can be found in Strayer et al (2001).

The interface is characterized by Coulomb sliding and/or tensile separation. It is designed in FLAC to model the geomechanics in which sliding or separation between planes is desirable, for example, joint, fault or bedding planes in a geologic medium. An interface has the properties of friction, cohesion, dilation, normal stiffness and shear stiffness, and tensile strength. The contact logic for either side of the interface is similar to that employed in the distinct element method (e.g., Cundall and Hart, 1992).

In this study, the elastic–viscous rheology constitutive law (Maxwell model) is used to simulate the tectonic transport patterns (material movement) of North and South Dabashan, and the interfaces are involved to simulate the strike-slip of the Bashan Arc fault. The elastic–plastic constitutive law (Mohr–Coulomb model) is also employed for pre-calculation. As for rigid tectonic units such as Bikou, Hannan, Foping, Wudang and Shennongjia, a set of rigid material properties are applied to make sure that they are hardly moved or deformed during the solving progress.

4. Model and results

4.1 Model design and grid generation

The Dabashan nappe thrusts are supposed to have suffered at least two stages of tectonic movements that are subduction collisional orogeny and subsequent intracontinental orogeny since Mesozoic-Cenozoic (Dong et al., 2006, 2008; Zhang et al., 2010). The subduction collisional orogeny results from the collisions between the North China Block, Qinling Micro-Plate and Yangtze Block along Shangdan and Mianlue sutures respectively (Cai et al., 1988; He et al., 1997; Zhang et al., 2001; Ratschbache et al., 2003; Wang et al., 2003; Dong et al., 2008), suggests that the model boundaries should be put to the north of Mianlue suture and to the south of the north margin of Yangtze Block (partly adapted according to the northeast margin of the Sichuan Basin). The intracontinental orogeny, as results of rock deformation under long term stress and temperature, is reflected by deformation and movement of finite difference grids inside the model and controlled by the constitutive model and material properties.

The east and west boundaries of the model are put to the east of Shennongjia terrane and to the west of Bikou terrane to make sure that all relevant tectonic units are involved in the model.

The Bashan Arc fault separates the North Dabashan and South Dabashan Belts into two different tectonic units (Dong et al., 2008). The tectonic orientation of the North Dabashan unit is NWW and almost parallel to that of the South Qinling Belt (about 290º– 300º, Dong et al., 2008). The tectonic orientation of the South Dabashan unit is more complex that may due to overprint by later tectonic actions (Dong et al., 2008). In this model, we design a NWW fault to represent the initial shape of the Bashan Arc fault.

Thus, the designed model skeleton consists of 8 sub-grids (Fig 4), in which the null grids (spaces that divided sub-grids) 1, 2, and 3 will be replaced by interfaces to represent the dividing line between North and South Dabashan, and the others (null grids) will be removed by merge and attach the related sub-grids together.

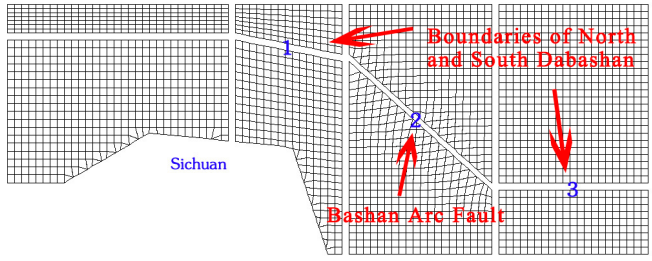

Figure 4. Skeleton of the plan-view model, maps the study area ranging N30.5º-33.5ºand E104º-112º. It extends about 900 km in W-E direction and 350 km in N-S direction, the average length of each finite difference grid equals to about 10 km in real study area. The model is initially built as sub-grids, null grids (marked as 1, 2, 3) represent boundaries of South and North Dabashan.

The other tectonic units such as Bikou Terrane, Hannan-micangshan Terrane, Foping Dome, Huangling-shennongjia Terrane, as well as Wudang Dome, playing role of rigid baffles, are added to the model during the experiment process. The completed plan-view model is shown in Fig. 3.

4.2 Boundary and initial conditions

The shape of the boundaries in the plan-view model is mainly based on a reconstructed and simplified map of the Dabashan and adjacent areas (Fig. 2), also consulted from a skeleton map published by He et al (1997). The north and southeast boundaries are designed as straight lines just for simplification. We tried applying declining boundaries along NEE and SE directions for north and southeast respectively as employed by Wu et al (2009), which did not make obvious difference to the modelling results.

Roll boundary conditions are applied to eastern and western boundaries along which the W-E movements are limited while the N-S movements are allowed. Free boundary conditions are added to the north and most of the south boundaries. To avoid unbalance failure leading by strong clockwise rotation, the corner segments of western and eastern of the south boundary are fixed.

A crustal shortening rate of 1.28 mm/year (He et al., 1997) is applied to both the north and south boundaries. This rate is approximately converted to a boundary stress of 1.1×10^{7} to 1.5×10^{7} Pa via pre-calculation with the plan-view model, which is also consistent with the boundary stress adopted in Wu et al (2009).

As a 2D plan-view model, the horizontal extrusion and plane displacement are mainly concerned while the initial gravity and stress applied inside finite difference mesh are set to default value of zero.

4.3 Constitutive model and material properties

Previous field and laboratory studies (He et al., 1997; Zhang et al., 2001; Dong et al., 2008; Wu et al., 2009; Wang et al., 2011, 2013) indicate that the Dabashan experienced long-term flexible deformation, therefore, large strain and viscous rheology constitutive law should be introduced for the simulation in this area (Wu et al., 2009). In this study, the classical viscoelasticity model (e.g. Maxwell substance) is adapted in the 2D plan-view model. The classical viscoelasticity model is widely used to simulate the time-dependent rock deformation, for example, intracontinental orogeny after collision. By carefully control the material properties, the classical viscoelasticity model can show behavior as either linear or non-linear viscous rheology. As a simple time-dependent constitutive model, it has been used in lots of previous numerical simulation studies in the fields of structural geology and tectonics (Dieterich and Carter, 1969; Treagus, 1973; Williams et al., 1978; Lin et al., 2004; Xia et al., 2006).

The material properties required for the classical viscoelasticity model are density, shear and bulk moduli (for the elastic behavior) and the viscosity (for the viscous behavior), which promise that the material flows continuously under an applied shear stress but behaves elastically under an applied isotropic stress (Itasca, 2005). In this study, we use a set of homogeneous material models for different tectonic units so that the effects of material difference can be tested and compared. The basic material model is consistent with the parameters for general average crust-lithosphere materials (e.g. Turcotte and Schubert, 1982) that include density of 2800 kg/m3, bulk modulus of 4×10^{10} Pa and shear modulus of 2.4×10^{10} Pa (Table. 1, Xia et al., 2006). As for the value of viscosity, a set of experiments is carried out to test the affect of material rheological properties which will be discussed in section of model results.

Table 1. The material properties of 2D plan-view model.

Table 1 The material properties of 2D plan-view model

Tectonic Units	Constitutive models	Density(kg/m^3)	Bulk moduli (Pa)	Shear moduli (Pa)	Viscosity (PaY)
North Dabashan	viscoelasticity	2800	4×10^{10}	2.4×10^{10}	1.6×10^{14}
South Dabashan	viscoelasticity	2800	4×10^{10}	2.4×10^{10}	1.6×10^{14}
Rigid units	viscoelasticity	2800	4×10^{10}	2.4×10^{10}	1.6×10^{16}

4.4 Model results

The 2D plan-view model is calculated under larger strain and in two stages. The first stage simulates the situation of "hard" collision in which the rock deformation behaviors are mainly elasticity by set the creep time-step to zero. When the first stage finished, we checked the maximum unbalance force in the system to make sure that the model system reached a mechanics balance state. The second stage simulates the situation of "inside" deformation in which the rock deformation behaviors are mainly viscous rheology that controlled by rock creep over a long period. For creep analysis, the time-step has realistic meaning other than a virtual calculating factor employed in other static analysis (Itasca, 2005). The creep time-step reflects the realistic period of rock deformation that should be determined by parameters of viscosity and shear moduli. In this study, we use an adjustable creep time-step that will be decreased whenever the maximum unbalanced force exceeds some threshold, and increased whenever it goes below some other level. By this way, we want to make sure that the model system is always under a mechanics balance state.

4.4.1 The pattern of materials movement in the Dabashan area

The first stage (instantaneous movement of materials under a "hard" collision) ended after 1774 static time-steps and reached a mechanics balance state. The contours plot of the displacement shows that the materials principally move towards south (Fig. 5a) and the displacement in the north Dabashan is larger than that in the south Dabashan.

There is small quantity of westward extrusion in the south Dabashan (Fig. 5b) and the maximum displacement in westward direction is about 20% compare to that in southward direction.

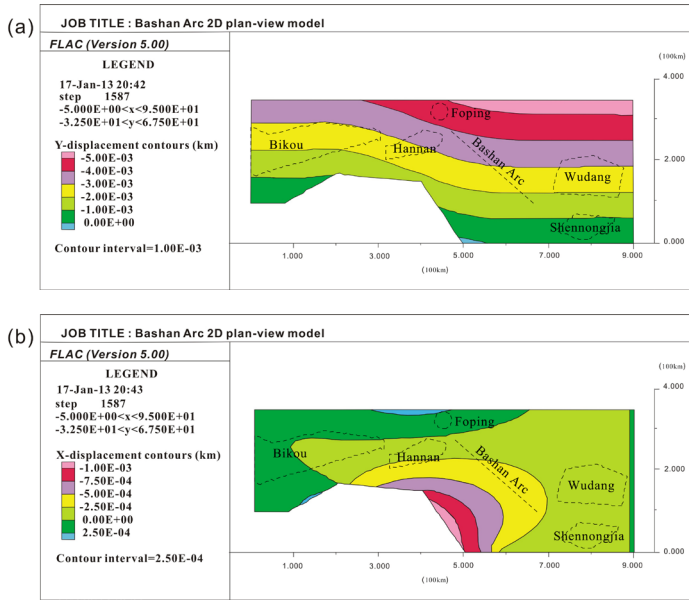

Figure 5. Displacement contours of the plan-view model at the end of "hard" collision. (a) Contours of the y-component of displacement (the maximum y-displacement is about 0.05 km). Positive values indicate northward movement and negative values indicate southward movements. (b) Contours of the x-component of displacements (the maximum x-displacement is about 0.01 km). Positive values indicate eastward movement and negative values indicate westward extrusion.

The second stage (creep of materials) falls into deformation failure due to some elements within the mesh become too strongly deformed and modelling cannot be continued. Fig. 6a shows the displacement pattern after 25 million years of collision. It can be clearly observed that the tectonic transport patterns (material movement) are characterized by strong NE-SW overthrust and the Bashan Arc fault (initialized as a straight line) shows an obvious arc shape extruded toward SW (240º) which is consistent with the present-day geomorphy in Dabashan area (Dong et al., 2008).

The NE-SW material movement can be more clearly analysed by plotting out the contours of the displacement component in the E-W and N-S directions, respectively. Fig. 6b shows the contours plot of the displacement component in the N-S direction (e.g. y-component) in which positive values indicate northward movements and negative values indicate southward movements. The maximum southward displacement of 30 km (negative contours) that distributes through the middle and the eastern part of Bashan Arc fault may reflect the overthrust nappe movement from north to south in tongue shape (e.g. the strong push in the middle and the weak push in the sides) that implies why the Bashan fault appears as an arc shape. The displacement toward the south in the South Dabashan unit is gradually smaller that may reflect that the deformation in the South Dabashan is gradually weakened from north to south (Dong et al., 2008).

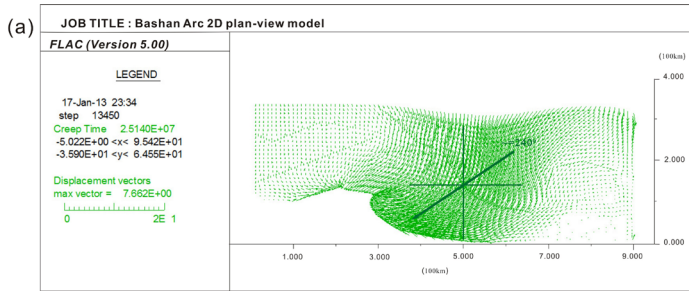

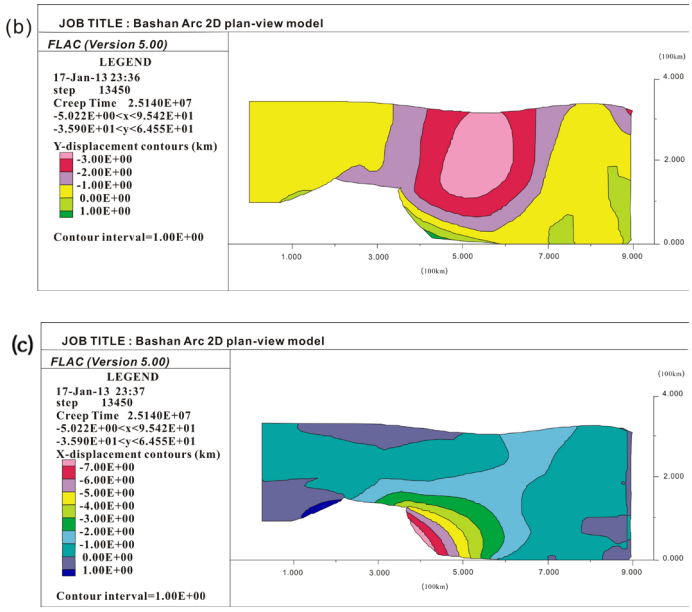

Figure 6. Results of the plan-view model. (a) Distribution of displacement vectors (the maximum displacement is about 76 km). (b) Contours of the y-component of displacement. Positive values indicate northward movement and negative values indicate southward movements. (c) Contours of the x-component of displacements. Positive values indicate eastward movement and negative values indicate westward extrusion.

We also notice that the areas surrounding Bikou-Hannan in the west and Wudang-Shennongjia in the east suffer minimum N-S displacement (the y-component is nearly zero) which implies an "anchor" effect of the Bikou-Hannan and Wudang-Shennongjia terranes.

Fig. 6c shows the contours plot of the displacement component in the E-W direction (e.g. x-component) in which positive values indicate eastward movements and negative values indicate westward movements. The trend of westward movements (negative contours) runs through the Dabashan area from north to south and the maximum westward displacement is at the South Dabashan unit.

The maximum displacement after 25 million years of collision is about 76 km (Fig. 6a). To compare with the published average crustal shortening distance of 40 km in the North Dabashan (Dong et al., 2008) and 64 km in the South Dabashan (He et al., 1997), a mark line AB is put into the model to track and calculate the average displacement in the North and South Dabashan units (Fig. 7), and the results are average displacement of 37 km and 41 km, maximum displacement of 39 km and 61 km for the North and South Dabashan (along AB path in Fig. 7), respectively. The potential underestimation of the values may be due to: 1) the 2D plan-view model could not include the slip and detachment layers beneath the Dabashan area that should be also contribute to the displacement; 2) the model only calculated 25 million years of the intracontinental orogeny that should be shorter than the actual situation. The larger deviation for the South Dabashan may also imply complex tectonic overprint in this area (Dong et al., 2008).

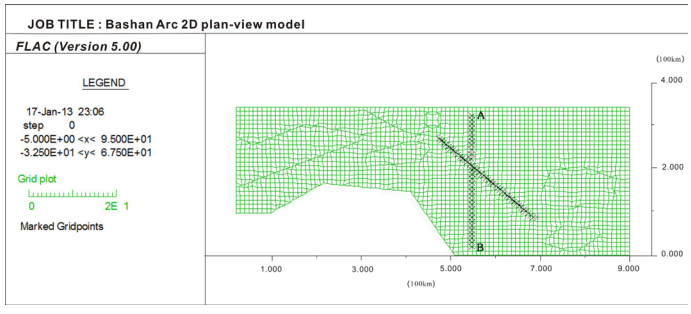

Figure 7. The marked path (AB) for calculating the average displacement in the North and South Dabashan

4.4.2 Dextral shear along the Bashan Arc fault

To evaluate whether the tectonic movement leading strike-slip along Bashan Arc fault, interfaces are introduced into the model to replace the initial marker lines for Bashan Arc fault (Fig. 4). The interfaces of 1 and 3 (in Fig. 4) represent the dividing line between north and south Dabashan and are limited neither to slip nor open, while the interface 2, representative of Bashan Arc fault, is allowed to slip or open by set relative small value to normal stiffness (kn) and shear stiffness (ks) parameters. The parameters for interface 1 are normal stiffness of 1×10^{10} Pa/m, shear stiffness of 1×1010 Pa/m and friction angle of 30º. These values are commonly used by Itasca (2005) and within the data range published by Kulhawy (1975), Rosso (1976) and Bandis et al (1983).

The fault slip experiment shows an obvious right-lateral shearing along Bashan Arc fault (Fig. 8b) compare with the initial finite difference grid (Fig. 8a) where the mark line AB is put on both side of the fault to track fault offset. As the parameter values for the interface are not derived from physical tests on real joints, the value of the fault offset can not reflect the realistic fault offset. What we concerned is the direction of the fault slip, yes, right-lateral shearing slip, which may imply that the right-lateral shearing produced by incongruous margin of block may play an important role on the formation of Bashan Arc (He et al., 1997).

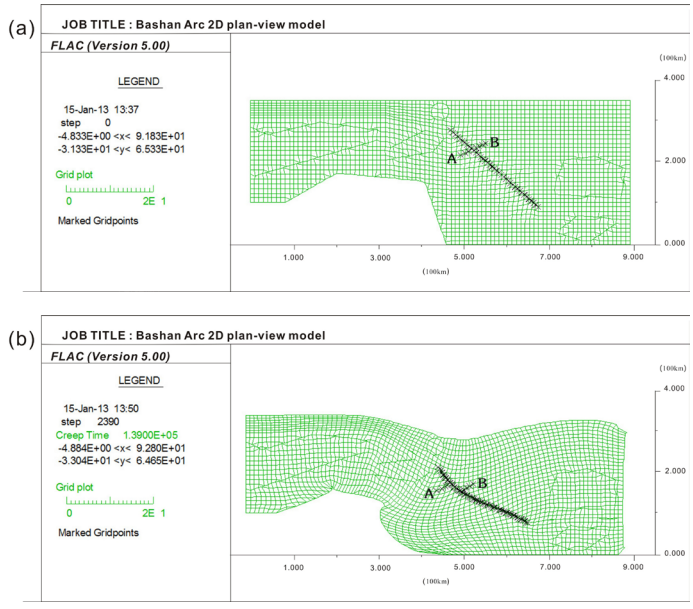

Figure 8. The right-lateral shearing of Bashan Arc fault. (a) Initial finite difference grids and the fault interface with a mark line AB. (b) Deformed finite difference grids and the fault interface with a mark line AB.

4.4.3 The effects of rigid "anchor"

Bikou, Hannan, Foping, Wudang, Shennongjia terranes are then removed from the initial model to estimate their contribution to bending of Bashan Arc, and the other conditions and parameters in the model keep consistent with that in the initial model. Fig. 9a and b show the contours plot of the displacement component in the N-S and E-W directions, respectively. A strong northward extrusion appears on the y-displacement contours plot (Fig. 9a) and maximum northward displacements take place in the area between Bikou and Hannan terranes. Taking into account of the strong southward extrusion in Dabashan area, the model may involve into clockwise whirl and out of balance. The x-displacement contours plot (Fig. 9b) indicates that westward extrusion seems nearly zero in North Dabashan unit that may be adverse to the formation of Bashan Arc. Therefore, "anchor" effects contributed by these rigid tectonic units should exist.

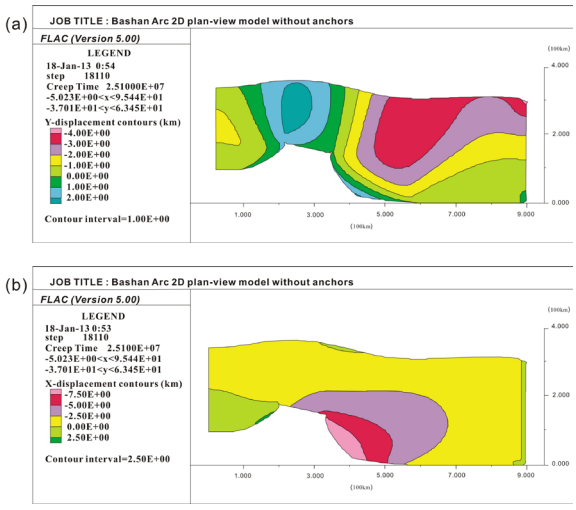

Figure 9. The "anchor" effects of Bikou, Hannan, Foping, Wudang, and Shennongjia. (a) Contours of the y-component of displacement. Positive values indicate northward movement and negative values indicate southward movements. (b) Contours of the x-component of displacements. Negative values indicate westward extrusion.

4.4.4. The rheological properties of rocks in the Dabashan area

The viscosity values for general average crust-lithosphere materials is about 5×10^{21} Pa s (Turcotte and Schubert, 1982; Xia et al., 2006) which is converted to 1.6×10^{14} Pa y because we use year as the unit for creep time. This value is used for both North and South Dabashan tectonic units in the 2D plan-view model, while Bikou, Hannan, Foping, Wudang, as well as Shennongjia terranes, a large value (more than 100 times of that for Dabashan) are employed to make sure that they are rigid compare to surrounding materials during creep analysis.

To estimate the relationship between viscosity values and deformation in Dabashan tectonic units, we tried a set of viscosity values for experiment. The results show that: 1) if the same viscosity value is set for the North and South Dabashan, the smaller the viscosity is, the larger the displacement obtained (Fig. 10a); 2) if the different viscosity values are set to the North and South Dabashan, enlarging the difference does not help to enlarge the displacement (Fig. 10b).

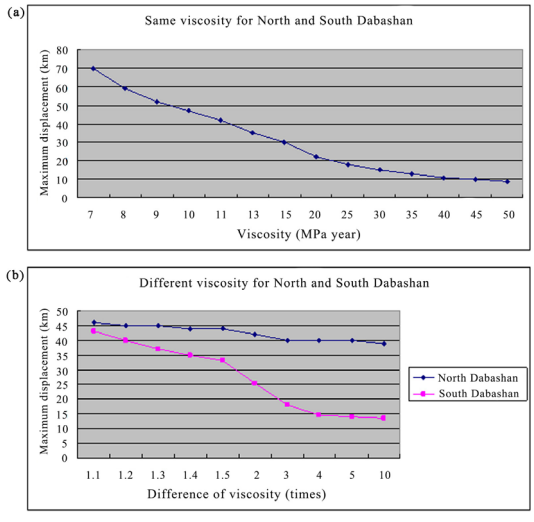

Figure 10. Sensibility analysis of the material viscosities. (a) The same viscosity value is set to both North and South Dabashan. The creep time is 10 million years after collision. (b) The different viscosity values are set to North and South Dabashan. The creep time is 10 million years after collision. The broken line of "North Dabashan" means an invariant viscosity (10 MPa year) for the South Dabashan and gradually enlarged viscosity for the North Dabashan; Accordingly, the broken line of "South Dabashan" means gradually enlarged viscosity for the South Dabashan while the North Dabashan keeping invariant.

4.5 Model limitations

This paper mainly focuses on 2D models for studying the geological and geodynamic condition of the Dabashan thrust structure using FLAC (2D) as main modeling tool. As general limitations of using 2D models for 3D orogenic deformation simulation, the model in this paper has below limitations:

1) Vertical topographical variation (Li et al., 2013) is not included in the model.
2) Viscosity of crustal and lithospheric rocks that depends on stress and temperature should be strongly vary with depth, is simplified as a few constant variables for different areas in this paper,
3) The Mianlue suture that affects the formation of the Dabashan thrust nappe, is not included in the model.

These limitations will be solved in our ongoing research with cross-view and 3D models.

5. Discussion

The formation of the Dabashan thrust nappe structure is acknowledged as results of multiple stage evolutions (He et al., 1999) that includes tectonic extension (Paleozoic), tectonic inversion (Middle Triassic) and thrust tectonics (Middle Triassic to Early Jurassic, Shi et al., 2012; Dong et al., 2006; Hu et al., 2009). After inter-continental collision orogeny (Late Triassic to Early Jurassic), Dabashan orocline continue reshaping during Late Jurassic to Early Cretaceous, proved by the sediment sequence and strata unconformity (Dong et al., 2005, 2006, 2008; Meng et al., 2005; Shi et al., 2007, 2012; Li et al., 2007; Qu et al., 2009; Zhang et al., 2010; Hu et al., 2012), isotopy dating (Cheng and Yang, 2009; Hu et al., 2009; Liu et al., 2011; Li et al., 2010, 2011, 2012, 2013), and apatite fission-track (Shen et al., 2009; Xu et al., 2010; Li et al., 2010, Shi et al., 2012; Hu et al., 2012).

Regarding to the key factors that affect and control the formation of the Dabashan thrust nappe, there are mainly four opinions: 1) the uplift at both ends of the Bashan Arc fault is main mechanism (Jiang et al., 1982; Guo et al., 1996; Wang et al., 2003; Zhang et al., 2004; Dong et al., 2010; Xu et al., 2010; Shi et al., 2012); 2) tectonic extension at the margin of paleo-contiental and irregular boundary are the decisive factors (Zhang et al., 2010), the dextral shear induced by the inconsistent morphology of the continental margins also plays a key role (He et al., 1997); 3) the arc-shaped fault that has been formed in the early stage of tectonic extension controls the thrust nappe developed toward southwest (Wang et al., 2011, 2013); 4) the detachment layers under Dabashan unit is the main formation condition (Wang et al., 2011, 2013).

From our study in this paper, it seems that the margin shapes generated by early tectonic extension (He et al., 1997, 1999) and the compression stress derived by subsequent tectonic inversion are important conditions to control the Meso-Cenozoic intracontinental orogeny, while pattern of materials movement in stage of thrust tectonics determines the formation of the Dabashan thrust nappe structure.

The results of the 2D plan-view models support that the shape of the north margin of Yangtze Block (e.g. the northeast margin of Sichuan basin extrusion northeastward against Qinling orogenic belt), together with the rigid Bikou-Hannan terrane on the northwest and Wudang-Shennongjia terrane on the southeast, are the main conditions of producing large-scale clockwise rotation in Dabashan area. During the movement of South Qinling towards south, the Bikou-Hannan terrane firstly obstructs locally the southward movements and compels the movement turn to eastward. The materials of eastward movement then conflict with the materials of southward movement at the north and west of the North Dabashan area, and change the direction to southward. The converged southward movements are then baffled by Wudang-Shennongjia terrane and turn to westward. Lastly, the materials of westward movement are blocked by the northward extrusion along the northeast margin of Sichuan basin, some of materials turn to north (thus the clockwise whirl is shaped) and the others turn to south along the east margin of Sichuan basin, as shown in Fig. 5a-b and 6a-c. The existence of the clockwise whirl is confirmed by right-lateral shearing along the Bashan Arc fault (shown in Fig. 8b).

The modelling results also reveal that the predominant pattern of materials movement through the Dabashan area is along an arc curve and pushes forward in a tongue-shaped in the front edge. The arc curve intersects with the Bashan Arc fault belt at the middle portion of the fault

belt that leads to the southwestward displacement in the middle portion is larger than that in the eastern and western portions of the fault belt thus the fault belt displays as a southwestward extrusion arc-shape (Fig. 6a).

As limitation of 2D plan-view model, the slip and detachment layers beneath the Dabashan area can not be simulated which may affect the estimation of the average displacement of the thrust nappe. However, the 2D plan-view model confirms that the N-S compression, dextral shearing, plus rock rheology can control the formation of the Dabashan thrust nappe structure.

6. Conclusion

According to the modelling results and discussion above, we propose following conclusions:

1) The compressive stress produced by the plate collision along north and south boundaries of the Dabashan tectonic unit is the main driving force;
2) The dextral shearing derived from the inconsistent shape on the block margins is the main controller;
3) Rigid tectonic units such as Bikou and Hanan-Micangshan terranes, Foping and Wudang dome, as well as Shennongjia-Huangling anticline contribute as "anchor" effects;
4) The rheology properties of rock material in the Dabashan area affect the shape of the arc. However, the difference of the rheology in the North and South Dabashan may not help to enlarge the deformation.

Acknowledgements

The authors would like to thanks reviewers for their constructive comments and suggestions. Financial support for this study was jointly provided by National Natural Science Foundation of China (grants: 41190074 and 40225008) and Most Special Fund (BJ081331) from the State Key Laboratory of Continental Dynamics, Northwest University.

References

Ames, L., Zhou, G.Z., Xiong, B.C., 1996. Geochronology and isotopic character of ultrahigh- pressure metamorphism with implications for collision of the Sino-Korean and Yangtze cratons, central China. Tectonics 15, 472–489.

Bader, T., Ratschbacher, L., Franz, L., Yang, Z., Hofmann, M., Linnemann, U., Yuan, H., 2013a. The heart of China revisited, I. Proterozoic tectonics of the Qin mountains in the core of supercontinent Rodinia. Tectonics 32, 661–687.

Bader, T., Franz, L., Ratschbacher, L., Capitani, C.d., Webb, A.A.G., Yang, Z., Pfänder, J.A., Hofmann, M., Linnemann, U., 2013b. The heart of China revisited: II Early Paleozoic (ultra)high-pressure and (ultra)high-temperature metamorphic Qinling orogenic collage. Tectonics 32, 922–947.

Bandis, S.C., Lumsden, A.C., Barton., N.R., 1983. Fundamentals of Rock Joint Deformation. Int. J. Rock Mech. Min. Sci. & Geomech. Abstr. 20, 249-268.

Cai, X.L., Wei, X.G., Wu, D.C., Hou, J.Y., 1988. Nappe structure patterns in the Wudang mountains. Journal of Chengdu University of Technology (Science & Technology Edition), 4, 30–39 (in Chinese with English abstract).

Cheng, W.Q., Yang, K.G., 2009. Structural evolution of Dabashan Mountain: evidence from ESR dating. Earth Science Frontiers 16 (3), 197-206 (in Chinese with English abstract).

Cundall, P.A., Board, M., 1988. Amicrocomputer program for modelling large-strain plasticity problems. Proceedings of the Sixth International Conference on Numerical methods in Geomechanics 6, pp. 2101–2108.

Cundall, P.A., Hart., R.D., 1992. Numerical Modeling of Discontinua. Engr. Comp. 9, 101-113.

Dieterich, J.H., Carter, N.L., 1969. Stress-history of folding. Am. J. Sci. 267, 129-154.

Dong, S.W., Hu, J.M., Li, S.Z., Shi, W., Gao, R., Liu, X.C., Xue, H.M., 2005. The Jurassic deformation in the Dabie Mountains and its tectonic significances. Acta Pet- rologica Sinica 21 (4), 1189-1194 (in Chinese with English abstract).

Dong, S., Hu, J., Cui, J., Meng, Q., Shi, W., Zhang, Z., Liu, G., 2006. Jurassic superposed folding and Jurassic foreland in the Daba Mountain,Central China. Acta Geoscientica Sinica 27, 403-410.

Dong, Y.P., Zha, X.F., Fu, M.Q., Zhang, Q., 2008. The structures of the Daba-shan fold-thrust belt, southern Qinling, China. Geological Bulletin of China 27, 1493–1508.

Dong, S. W., Shi, W., Zhang, Y. Q., et al., 2010. The Tectonic Stress Field in the Dabashan Orogen Resulting from Late Mesozoic Intra-Continental Orogeny. Acta Geoscientica Sinica, 31(6): 769–780 (in Chinese with English Abstract).

Dong, Y.P., Zhang, G.W., Hauzenberger, C., Neubauer, F., Yang, Z., Liu, X.M., 2011a. Palaeozoic tectonics and evolutionary history of the Qinling orogen: evidence from geochemistry and geochronology of ophiolite and related volcanic rocks. Lithos 122, 39–56.

Dong, Y.P., Zhang, G.W., Neubauer, F., Liu, X.M., Genser, J., Hauzenberger, C., 2011b. Tectonic evolution of the Qinling orogen, China: Review and synthesis. Journal of Asian Earth Sciences 41, 213-237.

Dong, Y.P., Genser, J., Neubauer, F., Zhang, G.W., Liu, X.M., Yang, Z., Heberer, B., 2011c. U–Pb and 40Ar/39Ar geochronological constraints on the exhumation history of the North Qinling terrane, China. Gondwana Research 19, 881–893.

Dong, Y.P., Liu, X.M., Santosh, M., Chen, Q., Zhang, X.N., Li, W., He, D.F., Zhang, G.W., 2012a. Neoproterozoic accretionary tectonics along the northwestern margin of the Yangtze Block, China: constraints from zircon U–Pb geochronology and geochemistry. Precambrian Research 196–197, 247–274.

Dong, Y.P., Liu, X.M., Zhang, G.W., Chen, Q., Zhang, X.N., Li, W., Yang, C., 2012b. Triassic diorites and granitoids in the Foping area: constraints on the conversion from sub- duction to collision in the Qinling orogen, China. Journal of Asian Earth Sciences 47, 123–142.

Dong, Y.P., Liu, X.M., Neubauer, F., Zhang, G.W., Tao, N., Zhang, Y.G., Zhang, X.N., Li, W., 2013. Timing of Paleozoic amalgamation between the North China and South China Blocks: evidence from detrital zircon U–Pb ages. Tectonophysics 586, 173–191.

Dong, Yunpeng, Santosh, M., 2016. Tectonic architecture and multiple orogeny of the Qinling Orogenic Belt, Central China. Gondwana Research, 29, 1-40.

Edmond, J.M., Paterson, M.S., 1972. Volume changes during the deformation of rocks at high pressures. Int. J. Rock Mech. Mining Sci 9, 161-182.

Enkin, R.J., Yang, Z., Chen, Y., Courtillot, V., 1992. Paleomagnetic constraints on the geodynamic history of the major blocks of China from Permian to the present. Journal of Geophysical Research 97, 13953–13989.

Faure, M., Lin, W., Le Breton, N., 2001. Where is the North China–South China block boundary in eastern China. Geology 29, 119–122.

Guo, Z., Deng, K., and Han, Y., 1996, Formation and Evolution of the Sichuan Basin: Beijing, Geologic Publishing House, 200 p.

Hacker, B.R., Ratschbacher, L., Webb, L., Ireland, T., Walker, D., Dong, S.W., 1998. U/Pb zir- con ages constrain the architecture of the ultrahigh-pressure Qinling–Dabie Orogen, China. Earth and Planetary Science Letters 161, 215–230.

He, J.K., Lu, H.F., Zhang, Q., Zhu, B., 1997. The thrust tectonics and it's transpressive geodynamics in Southern Dabashan Mountains. Geological Journal of China Universities 3, 419-428.

He, J.K., Lu, H.F., Zhu, B., 1999. The tectonic inversion and its geodynamic processes in northern Daba Mountains of eastern Qinling orogenic belt. Scientia Geologica Sinica, 34 (2) , 139–153.

Hobbs, B.E., Muhlhaus, H.B., Ord, A., 1990. Instability, softening and localisation of deformation. In: Knipe, R.J., Rutter, E.H. (Eds.), Deformation Mechanisms, Rheology and Tectonics. Geological Society of London Special Publication, pp. 143-165.

Hsu, K.J., Wang, Q.C., Li, J.L., Zhou, D., Sun, S., 1987. Tectonic evolution of Qinling moun- tains, China. Eclogae Geologicae Helvetiae 80, 735–752.

Hu, J.M., Shi, W., Qu, H.J., Chen, H., Wu, G.L., Tian, M., 2009. Mesozoic deformation of Dabashan curvilinear structural belt of Qinling structural belt. Earth Science Frontiers 16 (3), 49-68 (in Chinese with English abstract).

Hu, J.M., Chen, H., Qu, H.J., Wu, G.L., Yang, J.X., Zhang, Z.Y., 2012. Mesozoic defor- mations of the Dabashan in the southern Qinling orogen, central China. Journal of Asian Earth Sciences. 47, 171-184.

Huang, J.J., 2000. Research on the stress fields in superposed fold area e an example from Northeastern Sichuan. Scientia Geologica Sinica 35 (2), 140-150 (in Chinese with English abstract).

Itasca, 2005. FLAC: Fast Lagrangian Analysis of Continua, user manual, version 5.0. Itasca Consulting Group, Inc., Minneapolis.

Jiang, C., Zhizhi, Z., 1982. Qinling mountains orocline. In: Jiqing, H. (Ed.), Tectonic Structure in China and Nearby Region. Geology Publishing House, Beijing, pp. 102-114.

Jing, L., 2003. A reviewof techniques, advances and outstanding issues in numerical modelling for rock mechanics and rock engineering. International Journal of Rock Mechanics & Mining Sciences 40, 283-353.

Kröner, A., Zhang, G.W., Sun, Y., 1993. Granulites in the Tongbai Area, Qinling Belt, China: geochemistry, petrology, single zircon geochronology, and implications for the tec- tonic evolution of eastern Asia. Tectonics 12, 245–255.

Kulhawy, F.H., 1975. Stress Deformation Properties of Rock and Rock Discontinuities. Engineering Geology 9, 327-350.

Li, S.G., Xiao, Y.L., Liou, D.L., Chen, Y.Z., Ge, N.J., Zhang, Z.Q., Sun, S.S., Zhang, R.Y., Hart, S.R., Wang, S.S., 1993. Collision of the North China and Yangtze Blocks and formation of coesite-bearing eclogites: timing and processes. Chemical Geology 109, 89–111.

Li, Z., Liu, S., Luo, Y., 2006. Southern Dabashan foreland fold-thrust belt in central China. Geotectonics et Metallogenia 30, 294-304.

Li, S.Z., Kusky, T.M., Wang, L., Zhang, G.W., Lai, S.C., Liu, X.C., Dong, S.W., Zhao, G.C., 2007. Collision leading to multiple-stage large-scale extrusion in the Qinling orogen: insights from the Mianlue suture. Gondwana Research 12, 121-143.

Li, S.Z., Kusky, M.T., Zhao, G.C., Liu, X.C., Zhang, G.W., Kopp, H., Wang, L., 2010. Two-stage Triassic exhumation of HPeUHP terranes in the western Dabie orogen of China: constraints from structural geology. Tectonophysics 490, 267-293.

Li, Q.S., Gao, R., Wang, H.Y., Zhang, J.S., Li, P.W., Lu, Z.W., Guan, Y., Hou, H.S., 2011. Lithospsheric structure of northeastern Sichuan e Dabashan basin e range system and top-deep deformation coupling. Acta Petrologica Sinica 27 (3), 612-620 (in Chinese with English abstract).

Li, P.Y., Zhang, J.J., Guo, L., Yang, X.Y., 2012. Structural features and deformational ages of the northern Dabashan thrust belt. Geoscience Frontiers 3 (1), 41-49.

Li, Z.H., Xu, Z., Gerya, T., Burg, J.P., 2013. Collision of continental corner from 3-D numerical modeling. Earth and Planetary Science Letters 380, 98-111.

Li, N., Cheng, Y.J., Santosh, M., Pirajno, F., 2015. Compositional polarity of Triassic granit- oids in the Qinling Orogen, China: implication for termination of the northernmost paleo-Tethys. Gondwana Research 27, 244–257.

Lin, G., Wang, Y.H., Guo, F., Wang, Y.J., Fan, W.M., 2004. Geodynamic modeling of crustal deformation of the North China Block: a preliminary study. J. Geophys. Eng. 1, 63-69.

Liu, S., Li, Z., Liu, s., 2006. Formation and evolution of Dabashan foreland basin and fold- and thrust belt. Geological Publishing House, Beijing.

Liu, L.P., Li, S.Z., Liu, B., Liu, E.S., Dai, L.M., Zhang, G.W., 2011. Geometry and timing of Mesozoic deformation in the western part of the Xuefeng Tectonic Belt (South China): implication for intra-continental deformation. Journal of Asian Earth Sciences. 49, 330-338

Luo, S., Zeng, Q., Tu, T., Song, M., He, T., 2007. Tectonic modeling and seismic data tectonic interpretationin east Michangshan and west Dabashan front,Sichuan Basin Natural Gas Exploration & Development 3, 16-19.

Mattauer, M., Matte, P., Malavieille, J., Tapponnier, P., Maluski, H., Xu, Z., Lu, Y., Tang, Y., 1985. Tectonics of the Qinling belt: build up and evolution of eastern Asia. Nature 317, 496–500.

Meng, Q.R., Zhang, G.W., 1999. Timing of collision of the North and South China blocks: controversy and reconciliation. Geology 27, 123–126.

Meng, Q.R., Wang, E.C., Hu, J.M., 2005. Mesozoic sedimentary evolution of the northwest Sichuan basin: implication for continued clockwise rotation of the South China block. GSA Bulletin 117 (3e4), 396-410.

Okay, A.I., Sengör, A.M.C., 1993. Tectonics of an ultra-high pressure metamorphic terrane: the Dabie Shan/Tongbai Shan orogen, China. Tectonics 12, 1320–1334.

Ord, A., 1991. Deformation of rock: a pressure-sensitive, dilatant material. Pure Appl. Geophys 137, 337-366.

Qu, H.J., Hu, J.M., Cui, J.J., Wu, G.L., Tian, M., Shi, W., Zhao, S.L., 2009. Jurassic sedi- mentary filling process of Zigui basin in the eastern section of Daba Mountain tectonic belt and its structural evolution. Acta Geologica Sinica 83 (9), 1255-1268 (in Chinese with English abstract).

Ranalli, G., 1987. Rheology of the Earth. Allen and Unwin, London.

Ratschbacher, L., Hacker, B.R., Calvert, A., Webb, L.E., Grimmer, J.C., McWilliams, M.O., Ireland, T., Dong, S.W., Hu, J., 2003. Tectonics of the Qinling (Central China): tectonostratigraphy, geochronology, and deformation history. Tectonophysics 366, 1-53.

Ratschbacher, L., Franz, L., Enkelmann, E., Jonckeere, R., Poerschke, A., Hacker, B.R., Dong, S.W., Zhang, Y.Q., 2006. The Sino-Korean-Yangtze suture, the Huwan detachment, and the Paleozoic–Tertiary exhumation of (ultra)high-pressure rocks along the Tongbai–Xinxian–Dabie Mountains. Geological Society of America Special Publication 403, 45–75.

Ren, J.S., Zhang, Z.K., Niu, B.G., Liu, Z.G., 1986. On the Qinling Orogenic Belt-integration of the Sino-Korean and Yangtze Blocks, Qinling Orogenic Belt. Northwest University Press, Xi'an, pp. 99–110 (in Chinese with English abstract).

Rosso, R.S., 1976. A Comparison of Joint Stiffness Measurements in Direct Shear, Triaxial Compression, and In Situ. Int. J. Rock Mech. Min. Sci. & Geomech. Abstr. 13, 167-172.

Sengor, A.M.C., 1985. East Asia tectonic collage. Nature 318, 16–17.

Shen, C.B., Mei, L.F., Liu, Z.Q., Xu, S.H., 2009. Apatite and zircon fission track data, evidences for the Mesozoic Cenozoic uplift of Huangling dome, central China. Journal Mineral Petrologica 29 (2), 54-60 (in Chinese with English abstract).

Shi, W., Dong, S.W., Hu, J.M., Zhang, Z.Y., Liu, G., 2007. An analysis of superposed deformation and tectonic stress fields of the northern segment of Daba Mountain foreland. Acta Geologica Sinica 81 (10), 1314-1327 (in Chinese with English abstract).

Shi, W., Zhang, Y.Q., Dong, S.W., Hu, J.M., Wiesinger, M., Ratschbacher, L., Jonckheere, R., Li, J.H., Tian, M., Chen, H., Wu, G.L., Qu, H.J., Ma, L.C., Li, H.L., 2012. Intra-continental Dabashan orocline, southwestern Qinling, central China. Journal of Asian Earth Sciences 46, 20-38.

Shi, W., Li, J., Tian, M., Wu, G., 2013. Tectonic evolution of the Dabashan orocline, central China: Insights from the superposed folds in the eastern Dabashan foreland. Geoscience Frontiers 4, 729-741.

Strayer, L.M., Hudleston, P.J., Lorig, L.J., 2001. A numerical model of deformation and fluid-flow in an evolving thrust wedge. Tectonophysics 335, 121-145.

Tan, X.D., Kodama, K.P., Gilder, S., 2007. Paleomagnetic evidence and tectonic origin of clockwise rotations in the Yangtze fold belt, South China Block. Geophysical Journal International 168, 48-58.

Treagus, S.H., 1973. Buckling stability of a viscous single-layer system, oblique to the principal compression. Tectonophysics 19, 271-289.

Turcotte, D.L., Schubert, G., 1982. Geodynamics: Applications of Continuum Physics to Geological Problems. Wiley, New York.

Vermeer, P.A., De Borst, R., 1984. Non-associated plasticity for soils, concrete and rock. Heron 29, 1-64.

Wang, E., Meng, Q., Burchfiel, B.-C., Zhang, G., 2003. Mesozoic large-scale lateral extrusion, rotation, and uplift of the Tongbai-Dabie Shan Belt in East China. Geology 31, 307-310.

Wang, Z.C., Zhao, W.Z., Xu, A.N., Li, D.H., Cui, Y., 2006. Structure styles and their deformation mechanisms of Dabashan foreland thrust belt in the north of Sichuan basin. Geoscience 20 (3), 429-435 (in Chinese with English abstract).

Wang, R., Zhang, Y.Q., Xie, G., Xu, H., 2011. Origin of the Dabashan Foreland Salient Insights from Sandbox Modeling. Acta geologica sinica 85, 1410-1419.

Wang, B., Zhang, G., Yang, Z., 2013. New Mesozoic paleomagnetic results from the northeastern Sichuan basin and their implication. Tectonophysics 608, 418-427.

Williams, J.R., Lewis, R.W., Zienkiewicz, O.C., 1978. A finite-element analysis of the role of initial perturbations in the folding of a single viscous layer. Tectonophysics 45, 187-200.

Wu, H., Shi, W., Dong, S., Tian, M., 2009. A numerical simulating study of mechanical characteristic of superposed deformation in Daba Mountain Foreland. Earth Science Frontiers 16, 190-196.

Xia, B., Zhang, Y., Cui, X.J., Liu, B.M., Xie, J.H., Zhang, S.L., Lin, G., 2006. Understanding of the geological and geodynamic controls on the formation of the South China Sea: A numerical modelling approach. Journal of Geodynamics 42, 63-84.

Xu, Y.J., Yang, K.G., Ma, C.Q., 2005. Deformation Characteristics and the ESR Dating of Chengkou-Fangxian Fault Zone in the Qinling area. GEOSCIENCE 19.

Xu, Z.Q., Lu, Y.L., Tang, Y.Q., Zhang, Z., 1988. Formation of Composite Mountain Chains of the East Qinling–Deformation, Evolution and Plate Dynamics. China Environmental Science Press, Beijing, pp. 1–193.

Xu, C.H., Zhou, Z.Y., Chang, Y., Guillot, F., 2010. Genesis of Daba arcuate structural belt related to adjacent basement upheavals: constraints from fission-track and (U Th)/He thermochronology. Science in China (Earth Sciences) 53 (11), 1634-1646 (in Chinese with English abstract).

Yue, G.Y., Du, S.Q., Huang, J.J., Yang, W.N., 1996. Principle of Structural Compounding and Conjunction. Chengdu University of Science and Technology Press, Chengdu, pp. 15-42 (in Chinese).

Zhang, Y.R., 1985. The ancient Tongbai–Xinyang ophiolite zone and mélange. Regional Geology of China 13, 143–158 (in Chinese with English abstract).

Zhang, G.W., Mei, Z.C., Zhou, D.W., Sun, Y., Yu, Z.P., 1987. Formation and Evolution of the Qinling Orogenic Belt. Northwest University Press, Xi'an, pp. 1–191 (in Chinese with English abstract).

Zhang, G.W., Yu, Z.P., Sun, Y., Cheng, S.Y., He, B., Li, T.H., Xue, F., Zhang, C.L., 1989. The major suture zone of the Qinling orogenic belt. Journal of Southeast Asian Earth Sciences 3, 63–76.

Zhang, G.W., Meng, Q.R., Yu, Z.P., Sun, Y., Zhou, D.W., Guo, A.L., 1996a. Orogenesis and dynamics of Qinling orogen. Science in China (Series D) 26, 193–200.

Zhang, G.W., Zhang, B.R., Yuan, X.C., Xiao, Q.H., 2001. Qinling Orogenic Belt and Continental Dynamics. Science Press, Beijing, pp. 1–855.

Zhang, Y., Hobbs, B.E., Ord, A., Muhlhaus, H.-B., 1996b. Computer simulation of single layer buckling. J. Struct. Geol 18, 643-655.

Zhang, Y., Scheibner, E., Ord, A., Hobbs, B.E., 1996c. Numerical modelling of crustal stresses in the eastern Australian passive margin. Aust. J. Earth Sci. 43, 161-175.

Zhang, Y., Mancktelow, N., S., Hobbs, B.E., Ord, A., Muhlhaus, H.-B., 2000. Numerical modelling of single-layer folding: clarification of an issue regarding the effect of computer codes and the influence of initial irregularities. J. Struct. Geol. 22, 1511-1522.

Zhang, G.W., Dong, Y.P., Lai, S.C., 2004. Mianlue tectonic zone and Mianlue suture zone on southern margin of Qinling–Dabie orogenic belt. Science in China (Series D) 47, 300–316.

Zhang, Y., Shi, W., Li, J., Wang, R., Li, H., Dong, S., 2010. Formation Mechanism of the Dabashan Foreland Arc-Shaped Structural belt. Acta Geologica Sinica 84, 1300-1315.